

Alignment between Luminous Red Galaxies and surrounding structures at $z \sim 0.5$

Emilio Donoso^{1,2*}, Ana O’Mill³ & Diego G. Lambas^{3,4}

¹Universidad Nacional de San Juan, Av. Ignacio de la Roza 590(O), 5400 San Juan, Argentina

²Observatorio Astronomico Felix Aguilar, Av. Benavidez 8175(O), 5413 San Juan, Argentina

³IATE, Observatorio Astronomico de la Universidad Nacional de Cordoba, Laprida 851, 5000 Cordoba, Argentina

⁴Consejo de Investigaciones Cientificas y Técnicas (CONICET), Avenida Rivadavia 1917, C1033AAJ, Buenos Aires, Argentina

23 September 2018

ABSTRACT

We analyse a high redshift sample ($0.4 < z < 0.5$) of LRG’s extracted from the Sloan Digital Sky Survey Data Release 4 and their surrounding structures to explore the presence of alignment effects of these bright galaxies with neighbor objects. In order to avoid projection effects we compute photometric redshifts for galaxies within $3 h^{-1}$ Mpc in projection of LRGs and calculate the relative angle between the LRG major axis and the direction to neighbors within 1000 km/s. We find a clear signal of alignment between LRG orientations and the distribution of galaxies within $1.5 h^{-1}$ Mpc. The alignment effects are present only for the red population of tracers, LRG orientation is uncorrelated to the blue population of neighbor galaxies. These results add evidence to the alignment effects between primaries and satellites detected at low redshifts. We conclude that such alignments were already present at $z \sim 0.5$.

Key words: cosmology: theory - galaxies: formation - galaxies: alignment - galaxies: Large scale distribution

1 INTRODUCTION

The study of galaxy orientations has the potential to provide important information about the formation and evolution of cosmic structures. However, the interpretation of alignments, and particularly the search of its observational evidence, has a long confusing history. Bingelli (1982) introduced the idea of analyzing the distribution of orientations of clusters or their dominant galaxies relative to neighboring clusters or galaxies. Using a sample of well known Abel clusters he found that the position angle of first ranked galaxies strongly correlates with the orientation of the cluster itself, as determined from the spatial distribution of members. This author found that the orientation of a cluster is related to the distribution of neighboring clusters, i.e. clusters separated less than $\sim 30 h^{-1}$ Mpc tend to point to each other. Later, Struble and Peebles (1985) argued against this last effect claiming that it could be biased by systematic errors. In agreement with Bingelli (1982), Argyres et al. (1986) found that galaxy counts are systematically high along the line defined by the major axis of Abell clusters or its dominant member, up to at least $15 h^{-1}$ Mpc in projected distance.

Lambas et al. (1988) found that elliptical galaxies in the Uppsala General Catalog of Bright Galaxies showed a significant alignment signal up to $2 h^{-1}$ Mpc with respect to the surrounding galaxies identified by means of the Lick maps of galaxy counts, an effect

likely to be associated to anisotropy of large scales transferred to the elliptical galaxy population through mergers events. Since no similar correlation was found for spiral galaxies, this gave rise to the first detection of a morphology-orientation effect. Again, Rhee & Katgert (1987) and West (1989) found convincing evidence of Bingelli’s results, and with a large sample of rich Abell clusters, Lambas et al. (1990) obtained a 30% excess of brightest cluster galaxies pointing to the nearest-neighbor cluster at scales up to $15 h^{-1}$ Mpc. Also West (1989) presented evidence suggesting that the orientation of groups of galaxies in superclusters is not random, showing a strong correlation with surrounding groups within $\sim (15 - 30) h^{-1}$ Mpc.

More recently, such alignment effects have also been found by Yang et al. (2006), using a large sample of ~ 53.000 poor galaxy groups extracted from the New York University Value Added Galaxy Catalogue in the redshift range $0.01 < z < 0.2$. These authors determined that the distribution of satellite is aligned with the major axis of the brightest galaxies in groups. It is interesting to note that this systematic effect is statistically significant only for the red population of satellites and central galaxies.

From the theoretical point of view, numerical studies (West et al. 1991; van Haarlem & van de Weygaert 1993, Splinter et al. 1998; Faltenbacher et al. 2002) have shown that these cluster-cluster and substructure-cluster alignments occur naturally in hierarchical clustering scenarios for structure formation such as the Cold Dark Matter Model; a fact that can be interpreted as the result

* E-mail: edonoso@speedy.com.ar

of correlations of density fluctuations at different scales. Also, if galaxies formed after the collapse of their parent cluster, then the anisotropic initial conditions could be imprinted in member galaxy orientations, producing alignment effects. Both the tidal field of the parent cluster (Barnes & Efstathiou 1987, Usami & Fujimoto 1997), or an anisotropic merger scenario, (where interactions occur along the spatial directions corresponding to the primordial large-scale filaments) could explain the strong alignment between dominant galaxies and surrounding structures.

As previously discussed, evidence for the tendency of structures to align each other extends smoothly from the richest clusters of galaxies, to small groups and galaxies, over scales from Kpc up to several Mpc , providing a test for models of the origin and evolution of structure in the universe. All these works concern low redshifts, typically $z \lesssim 0.1$, and concentrate in rich and/or poor cluster environments. This limitation is not surprising since only a handful of high redshift clusters are known. Therefore, it is of interest to explore their presence in deeper samples.

The Luminous Red Galaxies (LRG) sample corresponds mostly to intermediate redshift ($0.2 \lesssim z \lesssim 0.55$) early type galaxies and, consequently, these objects may be ideal targets to test the alignment hypothesis at larger redshifts. A problem one faces with such a project is the lack of redshifts for the neighbor objects in projection that can dilute the alignment signals due mainly to contamination by distant background galaxies. In this paper, we use photometric redshifts calibrated with the publicly Artificial Neural Network code (Collister & Lahav (2004), ANNz). The galaxy training set used in the code from galaxy sample randomly selected the SDSS DR4 (main galaxy sample and LRGs). In this particular data set the rms redshift error in the range $z_s < 0.3$ is $\sigma_{rms} = 0.03$ (O'Mill et al. 2006, submitted) to estimate the redshifts of objects close in projection to the LRGs and compute the relative angle between the LRG position angle and the radius vector from the LRG position to that of each neighbor galaxy. The data and statistics are briefly described as well as the main results and conclusions.

2 DATA

The spectroscopic sample of the LRG used in this paper comprise the highest redshift objects of the total LRG sample. These galaxies were selected on the basis of color and magnitude to yield a sample of luminous intrinsically red galaxies (Eisenstein et al (2001)) that extends fainter than the SDSS galaxy spectroscopic sample.

Together, this sample of luminous red galaxies covers an enormous volume of space, about $1h^{-3} \text{ Gpc}^3$ when completed, and is expected to trace clusters of galaxies at higher distances while providing a fairly homogeneous population of galaxies suitable to study large-scale structure formation and giant elliptical evolution. The details of selection algorithms as well as its tune-up to remove the passive evolution of an old stellar population are explained in Eisenstein (2001).

SDSS photometry is accurate to $\sim 2\% rms$ in g,r,i bands; and $\sim 3\% rms$ in u and z . In the r band, a 95% completeness is achieved at $m_r \leq 22.2$. All magnitudes used in this work are modified Petrosian magnitudes (Blanton et al. (2001)), which measure galaxy fluxes within a circular aperture whose radius is determined by the azimuthally averaged light profile, and therefore measure a constant fraction of the total light independent of the position and distance. Spectroscopy is taken with two multifiber spectrographs that allow 640 spectra to be simultaneously acquired using pre-drilled aluminum plates. At a spectral resolution of 1800, the

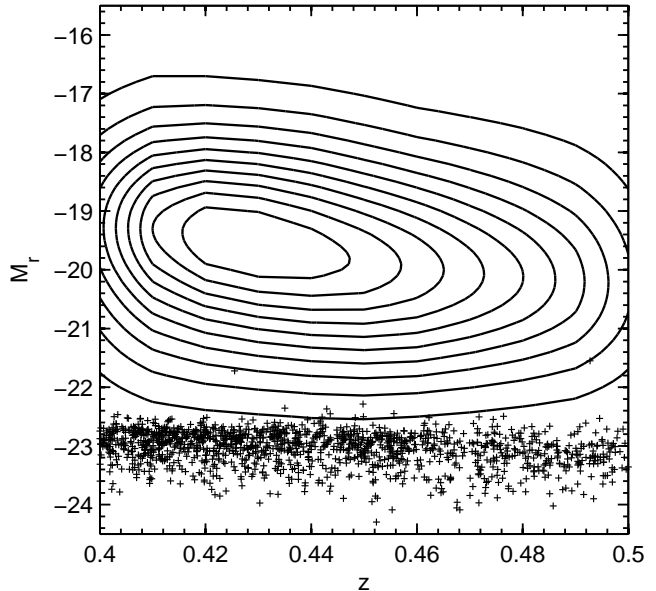


Figure 1. Petrosian absolute magnitude M_r vs redshift for ~ 25.000 tracer galaxies with photometrically derived redshifts calculated with the publicly available Artificial Neural Network code (Collister & Lahav (2004), ANNz). The ten contours enclose 10% – 100% respectively. The + signs correspond to the LRG sample.

typical signal-to-noise per pixel is > 4 at the peak of the g band. Redshift accuracy is 30 km/s . The fourth data release (DR4) covers a footprint area of 6670 and 4783 square degrees of sky for imaging and spectroscopy, respectively. A complete description of the survey is given by York et al. (2000).

Since we are interested in searching for alignment effects at the highest redshifts possible, we adopt the redshift range $0.4 < z < 0.5$ for the LRG targets. Position angle θ , major axis a and minor axis b of LRGs were derived by the *photo* reduction pipeline from the r band isophote at 25 magnitudes per square arcsec. Briefly explained, the radius of a particular isophote is measured as a function of angle and then expanded in Fourier series. Coefficients for this expansion are straightforward to calculate and account for the centroid, major and minor axis, and average radius of the isophote in question. After careful examination of LRG images provided by SDSS, we adopted a conservative range of galaxy flattening, $0.35 < b/a < 0.85$, for which misidentification, star contamination, and other problems are greatly reduced while keeping at the same time the highest number of objects and the lowest number of round shaped galaxies.

We have computed photometric redshifts using the ANNz code for all galaxies in fields centered on each LRG target within $\sim 2.5 h^{-1} \text{ Mpc}$. We applied k-corrections using the method of Blanton et al (2003), version 4.1.

In Figure 1, we show the distribution of redshifts and Petrosian absolute magnitudes of the spectroscopic LRG target sample, and of ~ 25.000 tracer galaxies with photometrically derived redshifts. It can be appreciated that LRGs are typically brighter by ~ 3.5 magnitudes than the most luminous galaxies in the fields.

3 ANALYSIS AND RESULTS

To search for alignment signals we calculate the relative angle ϕ between the position angle of the central luminous red galaxy and the vector pointing to each tracer galaxy within $1.5h^{-1}\text{Mpc}$ and $dv = 1000 \text{ km/s}$; and then count the number of galaxies in angular bins between 0° and 90° . For the quantification of the strength of these alignments we define the relative fraction distribution $f(\phi)$ as

$$f(\phi) = \frac{N(\phi) - \langle N(\phi) \rangle}{\langle N(\phi) \rangle}$$

where $N(\phi)$ is the number of galaxies at each angular bin and $\langle N(\phi) \rangle$ its mean value. This allows to effectively measure the fractional excess of tracer galaxy counts as a function of ϕ with respect to the mean. With this definition the absence of alignments would be characterized by a flat distribution around the zero mean. On the other hand, an excess of galaxy counts at low values of ϕ indicates the presence of an alignment effect.

In order to assess the statistical significance of alignments we adopt the following procedure:

(i) We compute the mean and dispersion of the relative angle ϕ between the LRG and the tracers. For an isotropic distribution is expected $\langle \phi \rangle \approx 45^\circ$ while any departure from this value indicates either alignments or anti-alignments.

(ii) We also calculate the distribution of $\delta = \langle \phi \rangle - 45^\circ$ which should exhibit for the isotropic case a mean value $\langle \delta \rangle \approx 0$ and standard deviation $\sigma = 90/\sqrt{12N}$, where N is the total number of LBG-galaxy pairs involved (Struble & Peebles (1985)). The mean and dispersion of these deviations across all galaxies in the sample allows us to construct $\chi^2 = \delta^2/\sigma^2$, which is another useful measure of the statistical significance of the results.

(iii) We fit the $f(\phi)$ distribution with $f(\phi) = b \cos(2\phi)$ and quote b values. This coefficient quantifies the anisotropy amplitude ($b > 0$ alignment, $b < 0$ anti-alignment).

(iv) We calculate the ratio between the number of ϕ values lesser (grater) than 45° and define $n_{45} = 2N_{<45}/N_{>45}$.

To address the question of how significant are the alignments signals detected we proceed as follows. We calculate the distribution of random occurrence of $\langle \phi \rangle$, b , and n_{45} using a Monte-Carlo method assigning random position angles to the central LRGs. By computing the statistics for 1000 random realizations we provide a robust estimate of the reliability of the results independently of a possible non-gaussian behavior. Also, since the galaxies used for each random sample are exactly the same as real data ones, with the same radial dependence, and the same physical properties; we can avoid any bias caused by clustering or other effects, leaving the LRG orientation as the only parameter that varies across the random set. Then, if an observed parameter value is well outside the corresponding distribution of the random realization we assure its reliability since it could hardly been obtained by chance. We compute the probability of obtaining values higher than the observed ones for $\langle \phi \rangle$, b and n_{45} , quoted in Table 1 as $P_{>}(\langle \phi \rangle)$, $P_{>}(b)$ and $P_{>}(n_{45})$, respectively. Low values of these probabilities indicate a strong confidence of the observed quantities being non-random.

We applied this set of statistical tests to our sample of LRGs and surrounding galaxies, and extracted different subsamples taking into account luminosity and color. We perform this analysis taking into account Yang et al. (2006) results, who found the red population to be more strongly aligned, an effect that is desired to be tested in the present analysis. By considering the tracer galaxy distributions of luminosity, shown in Figure 1, and $(g - r)$

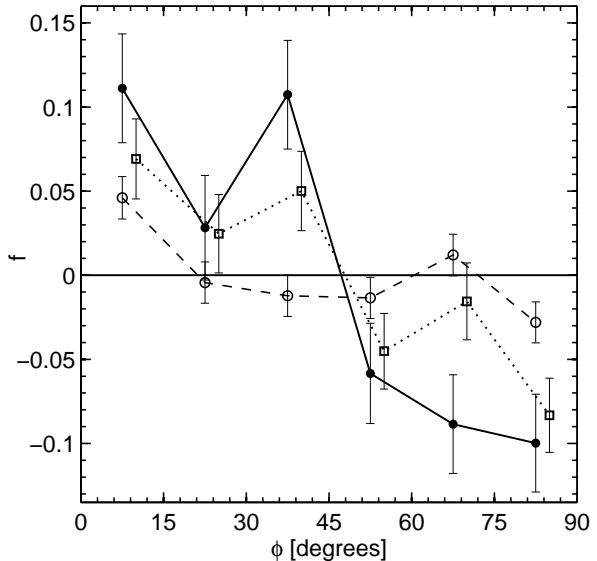


Figure 2. Normalized distribution of the relative angle Φ between LRGs position angle and the radius vector to neighbors within $rp \lesssim 1.5 h^{-1}\text{Mpc}$ and $dv = 1000 \text{ km/s}$. The dashed lines correspond to $M_r < -14$ (sample S), the dotted lines to sample S0 ($M_r < -14.0$ and $(g - r) > 1$), while the solid lines correspond to $M_r < -19.8$ and $(g - r) > 1$ (sample S1). In the case of no alignment we expect $f = 0$. It can be appreciated a significant alignment effect between luminous red galaxies and red neighbors (samples S0 and S1). Error bars correspond to Poisson statistical uncertainty.

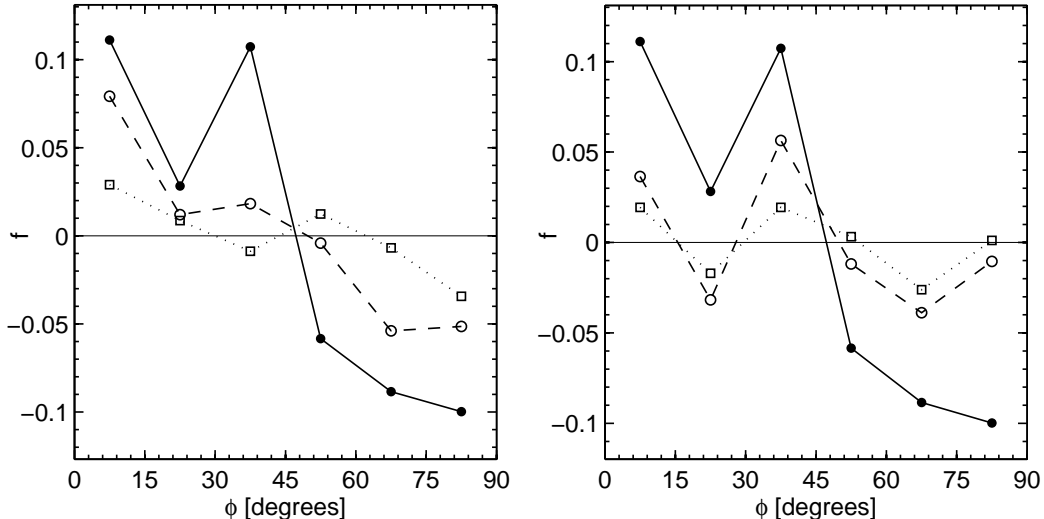
colour index, we have constructed samples of luminous (faint) tracers, $M_r < -19.8$ ($M_r > -19.8$); and red (blue) tracers with $(g - r) > 1$ ($(g - r) < 0.2$). In addition, we also analyzed complementary samples of bright (faint) LRGs, $M_r < -22.8$ ($M_r > -22.8$); with the same red (blue) population of tracers. All samples are defined in Table 1, conveniently labeled, and listed along with the obtained parameters of alignment and significance.

The results for samples S, S0 and S1 are shown in figure 2. There is a marginal alignment signal for sample S, while sample S0 has a larger and significant alignment amplitude. It is also clear that the most significant alignment signal is found for bright, red tracers (sample S1). This red bright population is strongly aligned as is evident by inspection to table 1. The magnitude of the effect is of the order of 11% as accounted by the amplitude of the cosine fit ($\langle \phi \rangle = 42^\circ.9$). Given the strong alignment detected for bright, red tracers, we have also explored for faint red tracers (sample S2) finding no significant alignment signal, as can be appreciated in table 1. So that, the alignment signal for sample S0 is likely to be due almost entirely to the bright galaxies of sample S1.

It is natural to expect a dependence between alignment effects and the velocity difference dv between central and surrounding tracer galaxies, so that an additional analysis is shown in figure 3, where the alignment signal and statistical parameters for sample S1 (bright red population) are plotted at several intervals of dv in the range $10^3 - 10^4 \text{ km/s}$. As expected, the alignment strength declines with increasing dv values as more uncorrelated tracers are included. This tendency is reflected also in the progression of $\langle \phi \rangle$ values towards isotropy at 45° and the lower values of χ^2 and alignment amplitude b . For $dv < 1000 \text{ km/s}$, the number of objects fall well beyond reasonable limits. Therefore, we adopt this limit value as the optimal one for the purposes of this analysis.

Table 1. Definition of samples and alignment statistics

Sample Name	LRG Magnitude	Tracer galaxies		σ	χ^2	$\langle \phi \rangle$	$P_{>}(\langle \phi \rangle)$	b	$P_{>}(b)$	n_{45}	$P_{>}(n_{45})$	N_{gal}
		Magnitude	Color									
S	$M_r < -21.5$	$M_r < -14.0$	no restriction	0.26	2.94	44.5	0.05	0.02	0.081	1.019	0.174	9883
S0	$M_r < -21.5$	$M_r < -14.0$	$(g - r) > 1.0$	0.49	7.00	43.7	0.002	0.066	0.002	1.100	0.006	2834
S1	$M_r < -21.5$	$M_r < -19.8$	$(g - r) > 1.0$	0.65	10.2	42.9	0.000	0.109	0.001	1.179	0.000	1593
S2	$M_r < -21.5$	$M_r > -19.8$	$(g - r) > 1.0$	0.73	0.14	44.7	0.36	0.011	0.400	1.008	0.462	1241
S3	$M_r < -21.5$	$M_r < -19.3$	$(g - r) < 0.2$	0.75	0.95	44.2	0.14	0.036	0.171	1.033	0.291	1210
S4	$M_r < -21.5$	$M_r > -19.3$	$(g - r) < 0.2$	1.01	0.05	45.2	0.42	-0.022	0.350	0.923	0.845	656
S5	$M_r < -22.8$	$M_r < -14.0$	$(g - r) > 1.0$	0.54	6.97	43.5	0.002	0.076	0.003	1.120	0.000	2241
S6	$M_r > -22.8$	$M_r < -14.0$	$(g - r) > 1.0$	1.06	0.42	44.3	0.26	0.031	0.293	1.031	0.365	593
S7	$M_r < -22.8$	$M_r < -14.0$	$(g - r) < 0.2$	0.69	0.21	44.6	0.29	0.008	0.380	0.959	0.769	1391
S8	$M_r > -22.9$	$M_r < -14.0$	$(g - r) < 0.2$	0.95	0.08	44.7	0.39	0.011	0.410	1.043	0.279	748

**Figure 3.** Alignment signal for sample S1 for different values of relative radial velocity difference dv between the central LRG and the surrounding tracers (left), and for different projected radius rp (right). The panel for dv shows how the relative excess of galaxy counts for $dv = 1000$ km/s (solid line), $dv = 3000$ km/s (dashed line) and $dv = 10000$ km/s (dotted line) gradually tending to isotropy. A similar tendency is shown in the right panel for values of $rp = 1.5 h^{-1} \text{Mpc}$ (solid line), $rp = 2.5 h^{-1} \text{Mpc}$ (dashed line) and $rp = 3 h^{-1} \text{Mpc}$ (dotted line).

In figure 4, we show the dependence of the alignment signal ($\langle \phi \rangle$, b , and χ^2) of sample S1 on relative velocity dv and projected separation (r_p). As it can be appreciated, there is a smooth tendency to isotropy as either dv and r_p increase.

In order to explore if the alignment effects comprising the red population extend to other type of galaxies we tested the alignment in two samples with both, bright and faint blue tracers (samples S3 and S4, respectively). As it can be appreciated in table 1, the results are fairly consistent with isotropy, implying no correlation between LRG orientation and blue late-type neighbors, a fact that is in good agreement with most previous investigations about alignments at low redshift (Yang et al. (2006)).

The question whether the luminosity of the central LRG affects the alignment pattern with neighboring galaxies is also worth to be investigated. For this matter, we repeated the analysis for samples of bright (faint) LRGs, with $M_r < -22.8$ ($M_r > -22.8$), and red tracers with $(g - r) > 1$ (samples S5 and S6, respectively). This indicates that the most significant alignment signal is obtained for bright LRGs even while considering red tracer galaxies. As the results described above suggest that color is a parameter that determines the presence or lack of correlation with the LRG

position angle, we performed the test again, but considering blue tracer ($(g - r) < 0.2$), with the same magnitude cut dividing bright and faint central LRGs (samples S7 and S8). The results indicate clearly that these cases are consistent with isotropy. Again, blue galaxy positions do not show correlation with LRG orientations, independently of their luminosity.

A visualization of the reliability of the results is given in the panels of figure 5 which show the distributions of occurrence of the alignment parameters ($\langle \phi \rangle$, n_{45} , and b) for the Monte-Carlo realizations with randomly assigned LRG's position angles for samples S1, S5 and S7. It can be appreciated that true value of the parameters for samples S1 and S5 are well beyond the Monte-Carlo simulation results indicating a statistically significant departure from isotropy. On the other hand, in sample S7 the observed values are well within the Monte-Carlo distributions.

4 CONCLUSIONS

From the statistical analysis applied to the data we may summarize the following results:

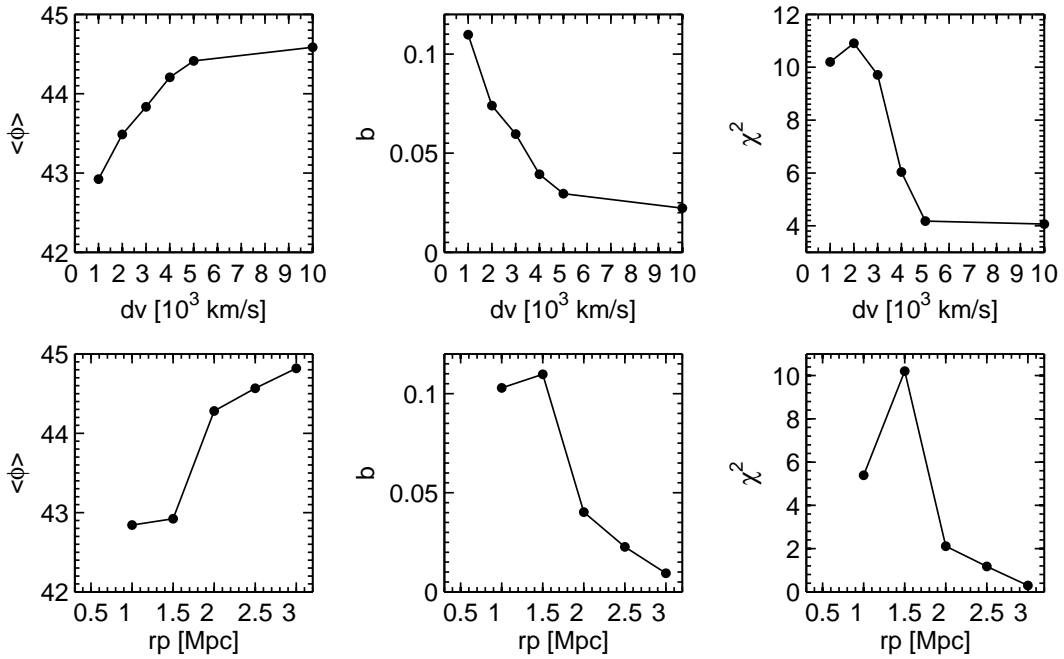


Figure 4. Dependence of $\langle \phi \rangle$, χ^2 and b on velocity difference (top row) and projected radius (bottom row) for sample S1. It is clear that for larger separations (in both velocity and projected radius) all parameters exhibit a behavior consistent with a gradual tendency to isotropy.

(i) A study of alignments equivalent to those typically performed at lower redshifts using information spectroscopic Catalogue can also be performed at higher redshifts, using distance estimates obtained via photometric redshift techniques. This allows to probe deeper into the universe, overcoming the natural limitation of wide-area redshift surveys.

(ii) The orientation of objects from the Luminous Red Galaxy sample extracted from the SDSS shows a significant alignment signal with respect to the direction to neighbors within $1.5 h^{-1} \text{Mpc}$ involving an excess of 11% galaxies respect to an uncorrelated population. This signal stands at over 3σ level only for the bright red population of tracer galaxies. The probability of obtaining such alignment pattern from 1000 random realizations is lesser than 1.

(iii) While the above tendency is quite remarkable for red, bright, neighbors, we found no evidence of such an effect for bluer and/or fainter galaxies around LRGs.

REFERENCES

Argyres, P. C., Groth, E. J., Peebles, P. J. E., & Struble, M. F. 1986, AJ, 91, 471
 Barnes, J., & Efstathiou, G. 1987, ApJ, 319, 575
 Binggeli, B. 1982, A&A, 107, 338
 Blanton, M. R., et al. 2003, AJ, 125, 2348
 Blanton, M. R., et al. 2001, AJ, 121, 2358
 Collister, A. A., & Lahav, O. 2004, PASP, 116, 345
 Eisenstein, D. J., et al. 2001, AJ, 122, 2267
 Faltenbacher, A., Kerscher, M., Gottlöber, S., & Mueller, M. 2002, A&A, 395, 1
 Lambas, D. G., Groth, E. J., & Peebles, P. J. E. 1988, AJ, 95, 996
 Lambas, D. G., Nicotra, M., Muriel, H., & Ruiz, L. 1990, AJ, 100, 1006
 O'Mill, Valotto & Lambas G. 2006, MNRAS, submitted
 Rhee, G., & Katgert, P. 1987, A&A, 183, 217

Splinter, R.J., Melott, A.L., Linn, A.M., Buck, C., & Tinker, J. 1997, AJ, 479, 632
 Struble, M. F., & Peebles, P. J. E. 1985, AJ, 90, 582
 Usami, M., & Fujimoto, M. 1997, ApJ, 487, 489
 van Haarlem, M., & van de Weygaert, R. 1993, ApJ, 418, 544
 West, M.J. 1989, ApJ, 344, 535
 West, M.J., Villumsen, J.V., Dekel, A. 1991, ApJ, 369, 287
 Yang, X., van den Bosch, F.C., Mo, H.J., Mao, S., Kang, X., Weinmann, S.M., Jing, Y.P., 2006, astro-ph/0601040
 York, D. G., et al. 2000, AJ, 120, 1579

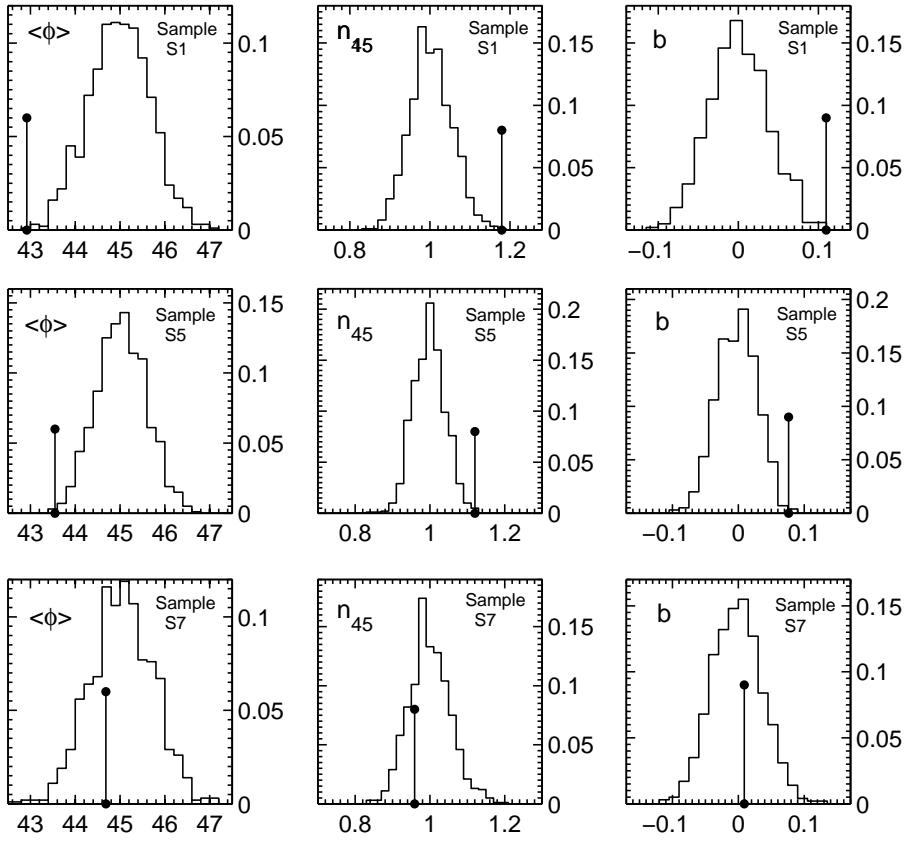


Figure 5. Distribution of statistical parameters $\langle\phi\rangle$, b and n_{45} drawn from 1000 samples where the LRG position angle θ is extracted from homogeneous distribution. Vertical lines indicate the values obtained directly from observed data for the different samples (see Table 1). The first row corresponds to the bright red population of tracer galaxies around LRGs, showing a significant alignment signal since by observed values are well outside the random distributions. The second row (sample S5, bright LRGs, red tracers) also show a correlation. The third row is a good example of no alignment effect consistent with isotropy corresponding to blue neighbors surrounding faint LRGs (sample S7).